

49th SME North American Manufacturing Research Conference, NAMRC 49, Ohio, USA

Stochastic Modeling for Tracking and Prediction of Gradual and Transient Battery Performance Degradation

Matthew B. Russell^a, Evan M. King^a, Chadwick A. Parrish^a, Peng Wang^{a,b,*}

^a*Department of Electrical and Computer Engineering, University of Kentucky, Lexington Kentucky*

^b*Department of Mechanical Engineering, University of Kentucky, Lexington Kentucky*

Abstract

As rechargeable battery-powered devices become a pervasive part of daily life, consumer standards for quality and reliability in these devices increase. One standard of particular interest is the ability to reliably track and predict the daily and lifetime capacity degradation of the batteries, over successive charge-discharge cycles. Tracking and predicting the degradation trend over batteries' entire service lives can be challenging, not only due to the nonlinear degradation patterns subject to different usage conditions, but also because of the presence of transient regeneration events that can rapidly increase the battery's maximum capacity and affect degradation rates. Current methods in the literature commonly apply an exponential model in a Bayesian inference framework to track and predict global degradation trend, neglecting the transient behaviors and local fluctuations, hence leading to unsatisfactory performance. This paper presents a new customary model specifically designed to track the gradual battery degradation pattern, combined with a Compound Poisson Process-based model that aims to capture the transient behaviors. The integration of the two parts, forming a comprehensive degradation model, provides a more accurate description of capacity variation throughout battery's life cycle. During the model training phase, upon historical data, parameters involved in the two models are estimated through two Bayesian inference techniques: step-by-step estimation by a Particle Filter and batch estimation by a Markov Chain Monte Carlo algorithm, with their performance compared. The estimated parameters are then utilized for generating transient events and predicting future capacity degradation. NASA's lithium-ion battery data are analyzed to evaluate the effectiveness of the developed degradation model.

© 2019 The Authors. Published by Elsevier B.V.

Peer review under the responsibility of the scientific committee of NAMRI/SME.

Keywords: Battery Health Prognosis; Degradation Modeling; Particle Filtering; Markov Chain Monte Carlo

1. Introduction

Accurate battery and power capacity modeling is critical in current product design, catalyzed by wireless devices and electric vehicle markets. As explained by Zhang et al. [1], proper battery modeling can have a significant impact on battery and its powered device in both efficiency and safety. Over time, the maximum capacity of batteries degrade due to gradual decrease in the electrolyte film thickness and increase in internal impedance. Battery capacity degradation is nonlinear and subject to varying usage patterns. Furthermore, a unique phenomenon known as battery capacity regeneration often occurs after a long rest period and can suddenly and significantly increase the capacity, complicating degradation analysis. Hence,

a typical battery capacity degradation curve includes two components: gradual (or global) degradation trends and transient (or local) regeneration events. Accurate and meaningful battery health prognosis requires comprehensive modeling of these two factors. Successful prognosis of degradation enables prediction of the battery's Remaining Useful Life (RUL), a valuable metric indicating how many charge-discharge cycles the battery can sustain before requiring replacement.

Predicting RUL for this degrading system requires a mathematical model to project the capacity trends into future cycles based on current and historical degradation characteristics. Gao et al. [2] have reviewed several techniques for system prognosis and RUL prediction that are relevant for lithium-ion battery degradation analysis. These models can be categorized based on the information used to build them. Physics-based models rely on a generalized mathematical representation of mechanisms underlying degradation behaviors, with the model parameters often determined experimentally [3]. Such a model may be unable to capture uncertainties associated with a specific instance of degradation and small variations in battery chemistry. In con-

* Corresponding author. Tel.: +1-859-562-2415

E-mail address: edward.wang@uky.edu (Peng Wang).

trast, data-driven models rely exclusively on historical system data without foundations in physical modeling, expressing future degradation as a function of past degradation and/or operating conditions in a black-box manner. Representative techniques for data-driven modeling include statistical regression, relevance vector machines [4], neural networks [5], and recent advances in deep learning [6]. These methods leverage large data sets and abstract most details of the physical system. Seeking to combine the advantages of the physical and data-driven approaches, hybrid models incorporate data-driven parameter estimation of the physically-informed modeling. Often, hybrid models can adapt to fluctuations in the degradation process while estimating uncertainty, representing the degradation and RUL by probability distributions.

Despite the wider success of these approaches, the limited volume of data and the absence of sophisticated physics-based lithium-ion battery degradation models has lead capacity prognosis research to frequently ignore the transient regeneration events. Hartman [7] develops a complex physics-based model for capturing the global degradation trend. While the parameters are fit using batch least squares estimation, a smoothing filter was applied to mitigate the influence of regeneration events on the global degradation trend. Starting from the electrochemical processes underlying battery degradation, [8] and [9] developed a model to characterize the degradation patterns, and introduced model parameters with certain physical meanings (e.g., impedance related factors), which were estimated by Relevance Vector Machines. The model was subsequently used in various parametric estimation frameworks, and particle filtering (PF)-based tracking yielded the most success. However, regeneration events were ignored in this model. Recognizing that gradual degradation rates changed over the battery's life cycle, Liu et al. [10] developed a piecewise autoregressive capacity model. Although this increased RUL prediction accuracy relative to single-mode modeling, different batteries would experience different changes in degradation rates, and a piecewise model designed for a certain battery struggles to generalize to others. To further improve the PF approach, Zhang et al. [11] explored the use of nonlinear-drifted fractional Brownian motion with PF but only estimated the battery RUL without future degradation curves projected. At the same time, Chen et al. (Chen2020) made different modifications to a PF framework, but similarly ignored the impacts of regeneration events. Therefore, while these approaches have achieved some success in estimating the battery RUL, the absence of regeneration event modeling prohibits the algorithms from creating realistic projected capacity degradation curves.

Incorporating the local regeneration events alongside the gradual degradation trends would clearly generate prognosis curves that are more representative of the observed behavior; however, such approaches introduce new challenges with model complexity. Wang and Gao [12] demonstrated a Local Search Particle Filter (LSPF) with an exponential model and a Total Variance (TV) filter for tracking both the global degradation trend via LSPF and detecting transient regeneration events using the TV filter. The TV filter enables the tracking algorithm to intelligently adjust when transient events are detected, reduc-

ing the negative impacts of regeneration events during tracking. However, while the TV filter can react to regeneration events as they occur, there is no mechanism for simulating regeneration events during prognosis, yielding inaccurate predicted future capacity curves. Zhang et al. [13] sought to explicitly include regeneration events in prognosis via a semi-Markov model that partitions the battery degradation into different segments: degradation and regeneration. By observing the relative frequency and time durations associated with regeneration events, a state transition matrix was created to describe the likelihood of transitioning between degradation and regeneration modes in successive steps. Observing that regeneration events may be captured by the higher frequency scales of a wavelet decomposition, [14] first applied wavelet transform to the entire battery curve and trained a nonlinear autoregressive neural network (NARNN) on cycles before prognosis began. The NARNN then recursively estimated the future multiscale components of the degradation curve before combining them for the final estimate. However, the practical applicability of this approach it unclear when full degradation curve is not available as a priori for wavelet decomposition.

Inspired by previous studies to develop a comprehensive, practical, and computationally efficient degradation model capable of realistic prognosis with regeneration events, this paper presents a stochastic degradation model that models regeneration events during prognosis, does not rely on information or data from future cycles, and efficiently characterizes variation in regeneration event magnitudes. To this end, a novel rational polynomial and a Compound Poisson Process (CPP) are combined to model global gradual degradation and transient regeneration phenomena, respectively. The stochastic rational polynomial model improves on previously used global exponential models by providing easily interpretable parameters and more accurately representing changes in the degradation rate at the end of the battery's life cycle. Furthermore, the inclusion of the CPP explicitly captures summary information about the frequency and magnitudes of regeneration events, facilitating simulation of transient capacity changes during the prognosis phase. In the initial data-driven training phase, the model parameters are estimated through two Bayesian inference techniques: step-by-step estimation by a Particle Filter and batch estimation by Markov Chain Monte Carlo, with their performance compared. The estimated parameters then guide the prediction of future gradual capacity degradation and transient events. NASA's lithium-ion battery data are analyzed to evaluate the effectiveness of the developed degradation model.

The rest of the paper is structured as follows: Section 2 introduces the mathematical models and theories behind both parametric estimation methods. Section 3 gives an overview of the NASA data to be analyzed, together with data pre-processing and the parameter estimation by two methods. Section 4 contains the full breadth of results for both methods, along with a discussion of their significance.

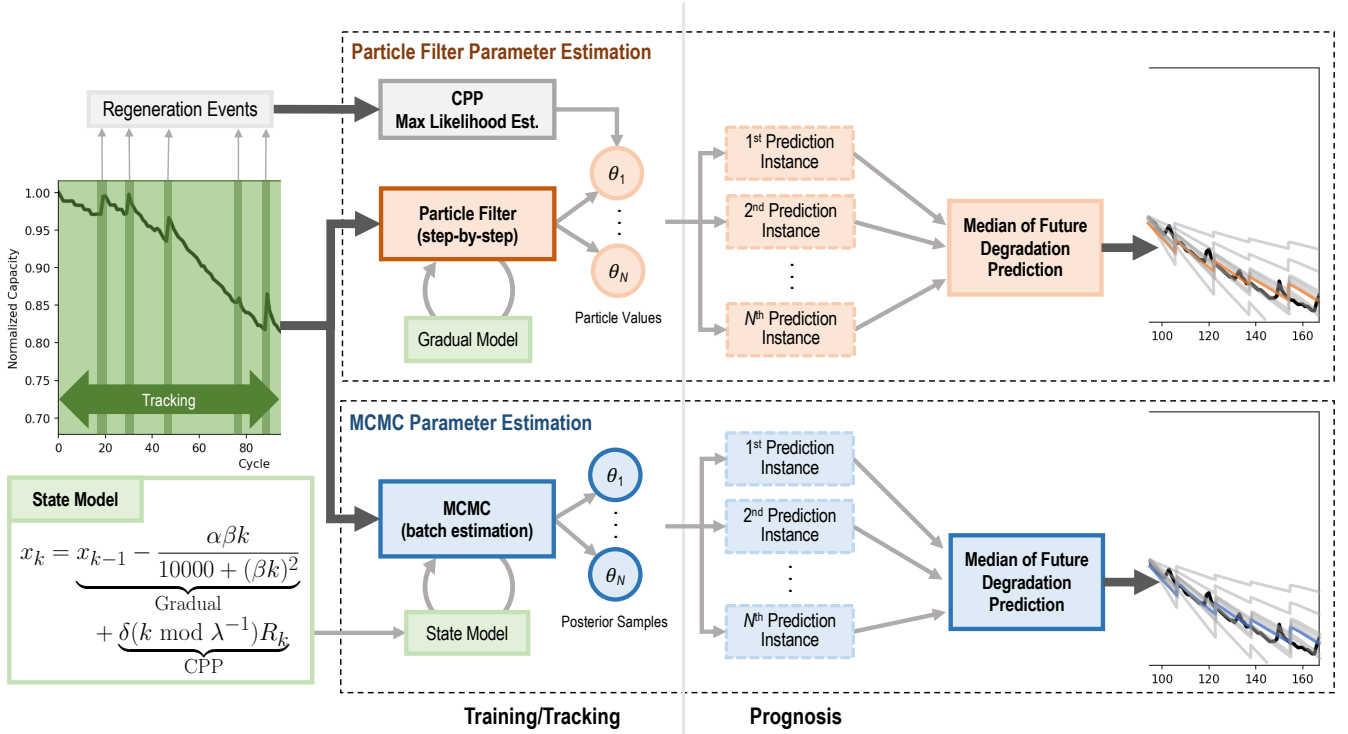


Fig. 1: Overview of stochastic modeling of gradual and transient lithium ion battery degradation using particle filtering and MCMC.

2. Stochastic Modeling Methods

Battery capacity degradation can be considered a stochastic process that includes gradual degradation and intermittent capacity regeneration events, with randomness caused by the battery's usage pattern, including rest time between charge-discharge cycles. The following sections describe two models for the two degradation components, including a novel rational polynomial model for gradual degradation compared to the commonly used exponential model, and a Compound Poisson Process (CPP)-based model for transient regeneration events. Particle filtering and Markov Chain Monte Carlo (MCMC), as two representative methods for stochastic parameter estimation, are also discussed. Particle filtering is a sequential Monte Carlo approach for step-by-step recursive parameter estimation, while MCMC estimates the distribution of parameters over a batch of observations. The theoretical foundations of both particle filtering and MCMC are summarized along with their application to capacity degradation modeling. Their performances are compared in Section IV. Fig. 1 presents an overview of the paper in a data processing order: formulation of the stochastic model and parameters involved, parameter estimation through two methods during the degradation tracking phase, and prognosis of future degradation and RUL.

2.1. Gradual Degradation Modeling

A popular model for gradual discharge and capacity degradation in lithium ion batteries uses the exponential function

[15, 16] and can be implemented in two ways. First, the battery capacity can be directly modeled as

$$x_k = ae^{bk} + ce^{dk} \quad (1)$$

where k is the charge cycle and a, b, c , and d are parameters to be estimated [17, 18]. However, depending on implementation, this model can result in prognosis curves that do not start from the actual capacity known at the end of tracking, creating a breakpoint between performance tracking and prediction. To remedy this, an alternative approach models step-by-step degradation through recursive capacity estimation using

$$x_k = x_{k-1} - Ce^{k^m} + v_p \quad (2)$$

where k is the charge cycle, C and m are parameters to be estimated via data-driven techniques from historical battery degradation measurements, and $v_p \sim N(0, \sigma_p^2)$ is the process noise [12]. Although capable of tracking the battery capacity, this model can suffer significant performance degradation when predicting future battery degradation. For example, unless the initial parameter ranges are chosen carefully over extremely tight ranges, the exponential will cause the cycle-to-cycle degradation to increase over time, in contrast to the actual degradation curve, which often exhibits a slowing degradation rate as the battery nears the end of life. While these initial ranges could be selected by fitting curves to the battery data ahead of time, such tight ranges can decrease the generalization capacity of the model. Therefore, while the exponential model could track degradation, it is found to be sensitive to the initial parameter ranges and easily able to produce prognosis curves that dis-

played sharply increasing rates of degradation or no degradation at all in latter cycles of the battery's life, both of which do not reflect the actual behavior of the battery.

Given these caveats of the exponential model, this paper develops an improved model that produced more realistic and accurate modeling of gradual capacity degradation towards the end of the battery's life cycle. Empirical inspection of battery degradation curves drives model development [15, 16] and revealed progressively increasing rates of degradation until approximately the 75th cycle before showing slightly shallower slopes after this point (see Fig. 2). As a result, an effective state transition model would produce slow degradation in the first few charge-discharge cycles, increased degradation rate in the middle section of the life cycles, and finish by returning to a slower rate at the end of the life cycles. Thus, the equation for degradation rate should start at zero, increase to some peak, and then decay towards zero as the battery reaches the end of its life. Furthermore, to overcome the parameter initialization challenge observed for exponential modeling and ensure computational efficiency, the model should have few parameters and be well-behaved across all combinations of these parameter values. For example, in a two-parameter model with parameter domains $\mathcal{D}_1 = [a, b]$ and $\mathcal{D}_2 = [c, d]$ for $a, b, c, d \in \mathbb{R}$, the model should not produce discontinuities or exploding values for any pair $(\alpha, \beta) \in \mathcal{D}_1 \times \mathcal{D}_2$. Furthermore, it is observed that an effective model would use comparable magnitude ranges for model parameters (e.g., of the same order) and not extend to very small or very large numbers (i.e., fall in the range $[10^{-2}, 10^2]$ for convenience).

With these constraints, several modifications to the exponential model have been investigated. However, the presence of the exponential function frequently made these model variations sensitive to parameter combinations that could result in exploding model values. Alternatively, a rational polynomial model with two free parameters is developed. Since the model for step-by-step degradation rate should pass through the origin (no degradation at cycle 0) and increase over the initial cycles, the expression would be directly proportional to k , the battery cycle. Also, the degradation rate should decay in the limit as k increases; thus, the degree of the denominator should exceed that of the numerator. Intuitively, this model's free parameters would control horizontal characteristics such as peak location, decay rate, and vertical scaling to fit the observed degradation flexibly. Satisfying these requirements, the new model for described gradual battery capacity degradation is defined as:

$$x_k = x_{k-1} - \frac{\alpha\beta k}{10000 + (\beta k)^2} + \nu_p \quad (3)$$

This rational polynomial model relies on two free parameters, α and β . Since the model is directly proportional to α , this parameter controls the vertical scaling of the degradation rate. Batteries that experience more rapid degradation over the entire life cycle will have larger values of α , while batteries that display slow degradation will be fitted to smaller values of α . The β parameter primarily controls the horizontal scaling and peak position of the degradation rate. Larger β values will increase the dominance of the denominator and cause the degradation

rate to decay more rapidly. Smaller values of β will stretch out the model horizontally, representing batteries that continue to maintain a higher rate of decay in the latter cycles of battery life. Including the product $\alpha\beta$ in the numerator ensures that changes to parameter β do not also dramatically affect the vertical scaling of the model.

2.2. Transient Degradation Modeling

Lithium-ion battery performance degradation demonstrates more complex patterns than just gradual degradation in an exponential way. After extended rest periods between two successive charge-discharge cycles, the battery chemistry experiences transient capacity regeneration events that significantly increase the capacity values. The exponential model and proposed rational polynomial model are not able to capture the regeneration events and resulting sudden changes in capacity. To comprehensively describe the mechanism underlying battery performance degradation and deliver accurate battery service life predictions, integration of the rational polynomial model with an additional model capable of capturing transient system behaviors is needed. As an artifact of rest periods, regeneration events would naturally exhibit correlation with battery usage patterns. Rarely cycled batteries would produce frequent regeneration events, while more heavily cycled cells would experience fewer rest periods necessary for regeneration phenomena. It is observed that while usage patterns may vary significantly among different batteries, the usage pattern for a single battery in a consistent operating environment would remain largely unchanged throughout its life cycle. In other words, the frequencies and magnitudes of capacity regeneration events would vary significantly for different batteries, but stay in a relatively constant range for a single battery throughout its service life. Therefore, a natural choice for modeling regeneration events is a Compound Poisson Process (CPP) [19]. A CPP describes a series of additive, Poissonian events drawn from identical distributions [20]. Although absent from existing battery models, CPP has proved capable of modeling non-deterministic degradation events in mechanical components and machines (e.g., abrupt bearing faults [21] and draught fan maintenance activities [20]) which are analogous to the regeneration events experienced by lithium-ion batteries. In the case of modeling battery regeneration effects, the CPP is defined as:

$$\Delta C_r(k) = \sum_{i=1}^{\lambda k} R_i \quad (4)$$

where $\Delta C_r(k)$ is the change in capacity resulting from regeneration events as of the k th charge-discharge cycle. The CPP is defined by the event frequency λ and the regeneration magnitude of the i th event R_i . While the regeneration frequency can be assumed to be a constant value for a specific battery, regeneration magnitudes are not constant but can be modeled by a Gamma distribution. Therefore, a comprehensive stochastic capacity model is obtained through combining the rational polynomial model and CPP model as

$$x_k = x_{k-1} - \frac{\alpha\beta k}{10000 + (\beta k)^2} + \delta(k \bmod \lambda^{-1})R_k + \nu_p \quad (5)$$

with

$$R_k \sim \text{Gamma}(s, \theta) \quad (6)$$

where s and θ are the scale and shape parameters of the Gamma distribution, to be fit using historical regeneration events. Process and modeling uncertainty is characterized through ν_p .

2.3. Parametric Estimation through PF

Particle filtering (PF) is a sequential Monte Carlo approach for sampling from an arbitrary, non-standard posterior distribution. For system tracking, this distribution represents the probability of k system state vectors $\mathbf{x}_{1:k}$ conditional on a set of k corresponding observations $\mathbf{y}_{1:k}$. The posterior distribution $p(\mathbf{x}_{1:k} | \mathbf{y}_{1:k})$ is estimated by a set of samples (i.e., particles) and corresponding weights that provide point estimates of the underlying posterior at the particle locations rather than fitting a standard distribution (i.e., multivariate Gaussian via Kalman filtering). This enables PF to model nonlinear, multimodal state distributions. Starting from particles initialized with certain distributions over the domain of the state and parameters to be estimated, PF recursively constructs posterior samples using a stochastic transition model that incorporates the system dynamics and process variation. Expected observations are generated according to a measurement equation and compared to actual sensing observations to score each particle based on its consistency with those observed values. This information is used to reweight the particles, assigning larger weights to those that closely match the observations and small or zero weights to those far from the true measurements. The range of particles preserved with non-zero weights is controlled by the measurement variance. This procedure will quickly drive most particle weights to zero as their state estimations diverge from the true system evolution, resulting in many unused particles and increasing the variance of the resulting estimation. Therefore, a critical final step during tracking is particle resampling. Particles are resampled according to their weights, moving dead particles (those with zero weights) to the location of more probable particles from the posterior distribution. Over time the particle estimates will converge to the parameter values which best model the system behavior as seen by the observations $\mathbf{y}_{1:k}$. Mathematically, using importance sampling, the expected value of an intractable posterior distribution (i.e., the distribution of system parameters) can be written in terms of an easily sampleable distribution $q(\mathbf{x}_{1:k})$ as:

$$\begin{aligned} \mathbb{E}[p(\mathbf{x}_{1:k} | \mathbf{y}_{1:k})] &= \mathbb{E}_{\mathbf{x}_{1:k} \sim q(\mathbf{x}_{1:k})} \left[\mathbf{x}_{1:k} \frac{p(\mathbf{x}_{1:k} | \mathbf{y}_{1:k})}{q(\mathbf{x}_{1:k})} \right] \\ &\approx \sum_{i=1}^N \mathbf{x}_{1:k}^{(i)} \frac{p(\mathbf{x}_{1:k}^{(i)} | \mathbf{y}_{1:k})}{q(\mathbf{x}_{1:k}^{(i)})} \end{aligned} \quad (7)$$

for N samples $\mathbf{x}_{1:k}^{(i)} \sim q(\mathbf{x}_{1:k})$, $i = 1, 2, \dots, N$ known as particles. For notational simplicity, for particle $\mathbf{x}_k^{(i)}$ we define weight

$$w_k^{(i)} = \frac{p(\mathbf{x}_{1:k}^{(i)} | \mathbf{y}_{1:k})}{q(\mathbf{x}_{1:k}^{(i)})} \quad (8)$$

with normalization constraint $\sum_{i=1}^N w_k^{(i)} = 1$. To leverage the recursive estimation of a sequential process, the posterior is assumed to follow a Markov system, leading to:

$$p(\mathbf{x}_{1:k} | \mathbf{y}_{1:k}) \propto p(\mathbf{x}_k | \mathbf{x}_{k-1}) p(\mathbf{y}_k | \mathbf{x}_k) p(\mathbf{x}_{1:k-1} | \mathbf{y}_{1:k-1}) \quad (9)$$

where $p(\mathbf{y}_k | \mathbf{x}_k)$ is the measurement distribution specifying the probability of observation \mathbf{y}_k being produced by the state value \mathbf{x}_k . Since $q(\mathbf{x}_{1:k})$ is an arbitrary distribution, the stochastic transition function $p(\mathbf{x}_k | \mathbf{x}_{k-1})$ of the dynamical system can be leveraged to select $q(\mathbf{x}_{1:k}) = p(\mathbf{x}_k | \mathbf{x}_{k-1})q(\mathbf{x}_{1:k-1})$ [22], and the weight update (within a normalization constant) can be rewritten as:

$$\begin{aligned} w_k^{(i)} &= \frac{p(\mathbf{x}_k^{(i)} | \mathbf{x}_{k-1}^{(i)}) p(\mathbf{y}_k | \mathbf{x}_k^{(i)}) p(\mathbf{x}_{1:k-1}^{(i)} | \mathbf{y}_{1:k-1})}{p(\mathbf{x}_k^{(i)} | \mathbf{x}_{k-1}^{(i)}) q(\mathbf{x}_{1:k-1}^{(i)})} \\ &= p(\mathbf{y}_k | \mathbf{x}_k^{(i)}) \frac{p(\mathbf{x}_{1:k}^{(i)} | \mathbf{y}_{1:k-1})}{q(\mathbf{x}_{1:k-1}^{(i)})} \\ &= p(\mathbf{y}_k | \mathbf{x}_k^{(i)}) w_{k-1}^{(i)} \end{aligned} \quad (10)$$

with samples $\mathbf{x}_{1:k}^{(i)}$ recursively generated from the stochastic system model $p(\mathbf{x}_k^{(i)} | \mathbf{x}_{k-1}^{(i)})$ for the k th step of the i th particle. To avoid a sparse set of particles with few nonzero weights, resampling is accomplished by treating the particle weights as the probabilities of a discrete distribution over $\mathbf{x}_{1:k}$, sampling N new particles, and resetting weights $w_k^{(i)} = \frac{1}{N}$.

When tracking the gradual degradation of lithium-ion batteries, the state consists of the battery capacity x and the model parameters α and β . In this framework, $\mathbf{x}_k = [x_k, \alpha_k, \beta_k]^\top$ and the single observed value y_k is the measured battery capacity. The sequential state samples are drawn from $p(\mathbf{x}_k | \mathbf{x}_{k-1})$ according to

$$\begin{aligned} x_k &= x_{k-1} - \frac{\alpha\beta k}{10000 + (\beta k)^2} + \nu_p \\ \alpha_k &= \alpha_{k-1} + \nu_\alpha \\ \beta_k &= \beta_{k-1} + \nu_\beta \end{aligned} \quad (11)$$

where ν_p , ν_α , and ν_β are the process noise samples all sampled independently from $\mathcal{N}(0, \sigma_p^2)$. The measurement distribution is defined as a Gaussian

$$p(y_k | x_k) = \mathcal{N}(x_k - y_k, \sigma_m^2) = \frac{1}{\sqrt{2\pi\sigma_m^2}} e^{-\frac{1}{2\sigma_m^2}(x_k - y_k)^2} \quad (12)$$

where σ_m^2 is the measurement variance. Therefore, the particle filtering weight update becomes

$$w_k^{(i)} = \frac{1}{\sqrt{2\pi\sigma_m^2}} e^{-\frac{1}{2\sigma_m^2}(x_k^{(i)} - y_k)^2} w_{k-1}^{(i)} \quad (13)$$

On the other side, the CPP parameter λ is computed in a separate framework before degradation tracking by PF, through a maximum likelihood estimation (MLE) over the K cycles' historical data before prognosis begins:

$$\lambda_{MLE} = \frac{N_r}{K} \quad (14)$$

where N_r is the number of regeneration events in the first K cycles. The regeneration magnitude distribution $p(R_k) = \text{Gamma}(s, \theta)$ is also fit using MLE over the set of regeneration event magnitudes occurring in the first K cycles. The regeneration events approximated by the CPP are then included into the

gradual model estimation by PF during the tracking phase. During prognosis, both gradual model parameters α and β and CPP model parameters are frozen, and Equation 5 is used to forecast the future battery capacity.

2.4. Parametric Estimation through MCMC

In contrast to PF, which decomposes the estimation of a sequential system to a combination of estimations of the individual posterior distribution, Markov Chain Monte Carlo (MCMC) offers a batch estimation alternative. Initializing a posterior sample using prior distributions over the model parameters, MCMC seeks to explore the posterior distribution by generating and conditionally accepting new candidate posterior samples from previously discovered posterior samples. Specifically, MCMC aims to construct a Markov chain with a stationary distribution that exactly matches the posterior. Thus, as the number of steps in the Markov chain grows large, the sequential samples generated appear to come from the target posterior, allowing for the model parameters to be estimated. To construct this stationary distribution, MCMC must satisfy the detailed balance equation:

$$q(\mathbf{x}_n \mid \mathbf{x}_{n+1})p(\mathbf{x}_{n+1}) = q(\mathbf{x}_{n+1} \mid \mathbf{x}_n)p(\mathbf{x}_n) \quad (15)$$

which implies the time-reversibility of the Markov process. That is, the probability of consecutive states \mathbf{x}_n and \mathbf{x}_{n+1} occurring in the forward Markov chain defined by $q(\mathbf{x}_{n+1} \mid \mathbf{x}_n)$ must equal the probability of consecutive states \mathbf{x}_{n+1} and \mathbf{x}_n occurring in the time-reversed Markov process defined by $q(\mathbf{x}_n \mid \mathbf{x}_{n+1})$. Popular approaches that satisfy the detailed balance equation include the Metropolis-Hastings algorithm [23] and Hamiltonian Monte Carlo (HMC) [24]. HMC outperforms Metropolis-Hastings by modeling the posterior sampling process using ideal Hamiltonian dynamics since the dynamics equations can be time-reversed [25]. In HMC, the dynamics equations allow quickly propagating the posterior samples throughout the posterior distribution. However, the nature of Hamiltonian dynamics risks the possibility of “U-turns” in which the end point of sample generation falls very close to the starting point, resulting in “wasted” samples that provides no new information about the posterior. The No U-Turn Sampler (NUTS) [26] algorithm provides a solution by propagating Hamiltonian dynamics while rejecting U-turn paths to consistently generate more informative samples to estimate the posterior, and hence it is used in this paper.

In the case of parameter estimation for modeling battery degradation, MCMC seeks to sample parameter sets $\boldsymbol{\theta} = [\alpha, \beta, \lambda, s, \theta]^T$ for the degradation model (Eq. 5) from the posterior distribution that specifies the probability of that parameter set generating the training observations. The posterior is then

$$p(\boldsymbol{\theta} \mid \mathbf{y}) \propto p(\boldsymbol{\theta})p(x_1)p(y_1 \mid x_1, \boldsymbol{\theta}) \prod_{k=2}^K p(y_k \mid x_k)p(x_k \mid x_{k-1}, \boldsymbol{\theta}) \quad (16)$$

where x_k is the state estimate at the k th cycle, $p(y_k \mid x_k)$ is the measurement probability (probability of state x_k generating observation y_k), and $p(x_k \mid x_{k-1}, \boldsymbol{\theta})$ is the state transition distribution from cycle $k - 1$ to k given parameters $\boldsymbol{\theta}$. Running MCMC

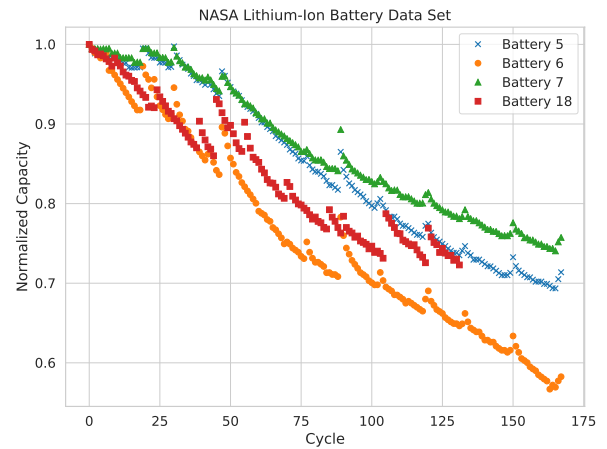


Fig. 2: NASA lithium-ion battery data set showing normalized capacity degradation for Batteries #5, #6, #7, and #18.

for a set of iterations will generate a set of parameter samples $\boldsymbol{\theta}$ from the posterior distribution representing combinations of model parameter values. Prognosis can then be conducted by propagating the capacity degradation model from the prognosis point using these sampled parameter values from the posterior. This produces a distribution of prognosis curves that describes the probable future evolution of the battery capacity. A key difference of the MCMC framework from the PF framework is that this method learns the regeneration parameters λ , s , and θ simultaneously with the gradual model parameters instead of estimating them separately through MLE.

3. Experimental Study

Experiments were performed on lithium-ion battery capacity degradation curves from NASA’s Prognostics Data Repository to evaluate the performance of the CPP model for regeneration events when model parameters are estimated through either particle filtering or MCMC.

3.1. NASA Battery Dataset

The lithium-ion battery degradation data set from NASA Ames Prognostics Data Repository [27] was used to evaluate the performance of the proposed algorithms. Each battery was cycled by charging to 4.2 V at a current of 1.5 A before discharging over a 2 A load until cell voltage reached 2.7 V [8]. Usage patterns (i.e., discharge curves and rest time) varied among batteries, and cycling was halted when the measured battery capacity reached 70% of the original capacity. Following previous studies [12], Batteries #5, #6, #7, and #18 (see Fig. 2) were used for testing the proposed methods. It is obvious that these batteries experienced multiple regeneration events throughout their service lives. Before training the degradation model, the battery capacity curves were normalized to start from 1.0, representing 100% initial capacity.

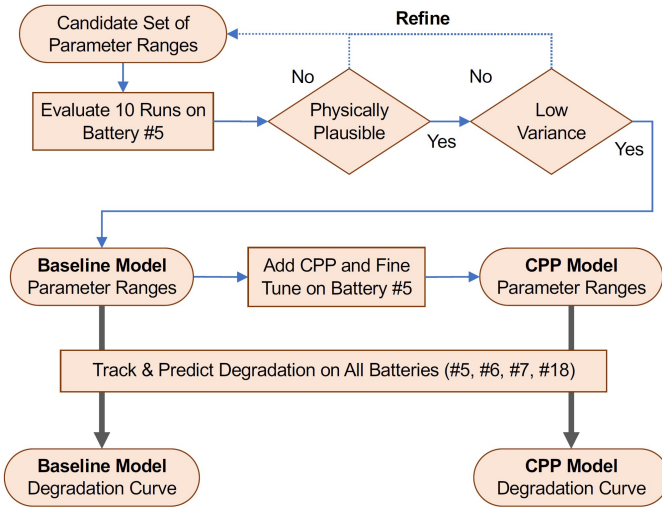


Fig. 3: Processing pipeline for selecting PF parameter ranges and MCMC parameter prior distributions for tracking and predicting battery degradation curves.

3.2. Data Preprocessing and Parameter Estimation

Fig. 3 summarizes the parameter initialization procedure before tracking and prediction of the degradation curves. The gradual degradation model from Eq. 3 contains two parameters that can be estimated using a step-by-step particle filter. Since the initial ranges of the particle values significantly affect the overall performance of the algorithm, a suite of preliminary tests were conducted to find initial parameter ranges that produced reasonable results, defined by clear tracking of actual battery curve in visual plots (i.e., prognosis curves have no unrealistic gradual increases in battery capacity) and low variance among runs. To this end, each preliminary test consisted of 10 runs of 2000 particles for prognosis after 75 cycles, and the initial parameter ranges were iteratively refined using the results. To prevent overfitting to the battery data, the initial ranges were only adjusted based on the algorithm's performance on Battery #5. The remaining three batteries were withheld to preserve the integrity of the complete results. This procedure resulted in the following initial parameter distributions for the gradual model without CPP (Eq. 3):

$$\begin{aligned} x &\sim U(0.95, 1.05) \\ \alpha &\sim U(0.5, 1.0) \\ \beta &\sim U(1.5, 3.5) \end{aligned} \quad (17)$$

and for the gradual model with CPP (Eq. 5):

$$\begin{aligned} x &\sim U(0.95, 1.05) \\ \alpha &\sim U(0.5, 1.0) \\ \beta &\sim U(0.25, 2.25) \end{aligned} \quad (18)$$

The only change in range is for the β parameter which controls how quickly the capacity degradation rate decays. The β values are higher for the model without CPP (resulting in shallower capacity curve slopes) since the gradual degradation model must reduce the degradation rate in later cycles to offset the increase

in capacity caused by regeneration events. The preliminary trials indicated that effective noise parameters (used for Eq. 5 and Eq. 13) for both cases were:

$$\begin{aligned} \sigma_p^2 &= 10^{-4} \\ \sigma_m^2 &= 5 \times 10^{-5} \end{aligned} \quad (19)$$

where σ_p^2 is the process variance used for all estimated parameters, and σ_m^2 is the measurement variance for the capacity value.

When using MCMC, the comprehensive stochastic capacity model from Eq. 5 describes all five parameters that are estimated simultaneously. A large range of initial parameter priors was first tested and then refined down like the PF case to produce a tighter distribution of outputs and realistic degradation trends. Each preliminary test was done using 100 iterations of “burn-in” (to improve model convergence) and 100 iterations of training. As with PF, this training was performed using the first 75 points of capacity data for Battery #5. This procedure resulted in the following distributions for the MCMC parameters without CPP:

$$\begin{aligned} \alpha &\sim U(0.2, 1.0) \\ \beta &\sim U(2.0, 2.3) \end{aligned} \quad (20)$$

and the following parameters with CPP:

$$\begin{aligned} \alpha &\sim U(0.7, 1.7) \\ \beta &\sim U(2.1, 3.6) \\ \lambda &\sim U(0.02, 0.1) \\ s &\sim U(1.001, 2.0) \\ \theta &\sim U(0.001, 0.0175) \end{aligned} \quad (21)$$

The preliminary trials indicated an effective noise value was

$$\sigma_m^2 = 0.75 \quad (22)$$

where σ_m^2 is the measurement variance of the capacity value.

Once these initial parameter ranges were identified for PF and MCMC, parameter estimation, degradation tracking, and prognosis were accomplished as indicated in Fig. 1. PF estimation was performed by testing each battery with and without the CPP model. Each configuration ran for 100 Monte Carlo trials of 1000 particles. Capacity prognosis was evaluated after tracking for 75 and 100 cycles, and the median prognosis curve was used to evaluate the prediction to prevent outlier particles from distorting performance metrics. Since particle filtering is a step-by-step estimation method, the CPP parameters λ and Gamma distribution parameters s and θ were separating selected via maximum likelihood estimation over the capacity curve values preceding the start of prognosis (as shown in Fig. 1).

When implementing MCMC, each battery was again tested with and without the CPP model, with each model running for 1000 burn-in iterations and 1000 training iterations. Capacity prognosis was again performed for 75 cycles and 100 cycles of training data. The median curve was generated by running prognosis with the median parameter values from the MCMC samples 1000 times, sampling different regeneration magnitudes during each trial. The mean of these Monte Carlo trials then represents the expected curve generated by the set median parameter values (i.e., the median prognosis curve).

4. Results

Figs. 5–8 present the PF and MCMC tracking results with prognosis after 75 and 100 cycles for each of Battery #5, Battery #6, Battery #7, and Battery #18, respectively. MCMC results for the same configuration (i.e., same battery, prognosis point, and model) are shown directly below the PF results for comparison. Furthermore, Fig. 4 provides a representative example of the shortcomings of the exponential-based gradual model used in similar studies, illustrating the unrealistic degradation curves when applied via PF to Battery #5 for prognosis after 75 cycles.

4.1. Tracking and Prediction through PF

The degradation tracking and prediction results through PF-based parameter estimation are shown on the first and third rows of Figs. 5–8. Two prognosis cases are demonstrated in these figures, one using data from the first 75 cycles for tracking, and the other using data from the first 100 cycles for tracking. Tracking and prediction made by gradual model only and model with CPP are included in both cases. Overall, the gradual model tracks the degradation well. However, as expected, the regeneration events with large amplitudes (e.g., near the 50th cycle of Battery #6) lead to discrepancies between tracking and actual degradation, which then take several cycles for the tracking to recover and re-follow the actual degradation trajectory. For gradual model only based prognosis after 75 cycles the medians of the prediction distributions are off the actual degradation trajectories for Battery #6, #7, #18. Also, only Battery #5 and Battery #7's 90% prediction intervals cover the actual degradation trajectories. Prognosis after 100 cycles is better than the prognosis after 75 cycles, as expected, since more data have been used to estimate the model parameters. While the prediction intervals narrow, only Battery #18's degradation curve is not fully covered by the prediction interval, as this battery experienced two large regeneration events after 100 cycles.

Prognosis based on the model with CPP does not improve the results as significantly as expected. In the case of prognosis after 75 cycles, the medians of prediction distributions still miss the actual trajectories for Battery #6, #7, #18. However, it is observed that the 90% prediction intervals cover all actual trajectories for all batteries, which is a promising indicator. The same observations are confirmed in the case of prognosis after 100 cycles. On the other hand, a quantitative measure, root mean squared error (RMSE), is used to further evaluate the prognosis performance, as shown in Fig. 9. The results indicate that the combination of the gradual model and CPP model do not perform (as expected) better than the gradual model only, which will be discussed in Section 5.

Fig. 10 presents examples of step-by-step estimation results for model parameters α and β during a trial with prognosis after 75 cycles. While the gradual model only and the model with CPP obtain similar estimation distributions for the α parameter, the obtained distributions for β are different. As explained above, the β values are expected to be higher for the model without CPP since the gradual degradation model must reduce the

degradation rate in later cycles to offset the increase in capacity caused by regeneration events. Once tracking and estimation are complete, the parameter values are frozen and used for prediction.

4.2. Prediction through MCMC

The degradation tracking and prediction results through MCMC-based parameter estimation are shown on the second and fourth rows of Figs. 5–8. For prognosis based on the gradual model only, prognosis by MCMC outperforms the prognosis by PF, with only prognosis after 100 cycles for Battery #18 missing the actual degradation. For some cases, such as prognosis after 75 cycles for Battery #6 and #7, although the prognosis could miss one regeneration event with a large amplitude, the 90% prediction interval covers most parts of actual degradation trajectories.

For prognosis based on the model with CPP, the prediction curves visually look more similar to actual degradation trajectories than predictions by gradual model only. Furthermore, the generation of regeneration events during prognosis enables comparable or better performance than prognosis without CPP. For example, in prognosis after 75 cycles, the model with CPP achieves a minimum RMSE on the unseen batteries of 0.0317 on Battery #7 compared to a minimum RMSE of 0.0318 from the gradual model only. For prognosis after 100 cycles, the CPP model proves more advantageous and achieves a minimum RMSE of 0.0116 on Battery #7 in contrast to the minimum RMSE of 0.0146 from the gradual model only.

5. Discussion

5.1. Exponential Model vs. Developed Gradual Model vs. Model with CPP

Compared to the commonly adopted exponential model, the developed gradual model in the form of a rational polynomial demonstrates better performance as expected, as shown in Fig. 9. This is because the developed gradual model could generate a lower degradation rate for the prognosis towards the end of battery life.

In the prognosis by PF, predictions by the model with CPP are not better as expected than the predictions by the gradual model only, when RMSE is utilized to quantify the prognosis results. The reasons are twofold. First, in the PF implementation, the regeneration events in terms of frequency and amplitudes are estimated through data preprocessing, out of the loop of system tracking by PF. This would cause the regeneration events to be generated at different time points than when the actual events occur. The mismatch of the regeneration event occurrence time led to a mismatch between the actual degradation trajectories and medians of predictions, resulting in a higher RMSE. Second, RMSE is only used to evaluate the medians of predictions, and it is unable to evaluate other perspectives of the prediction results, for example, whether the actual trajectories stay within the prediction intervals. Apparently, the latter

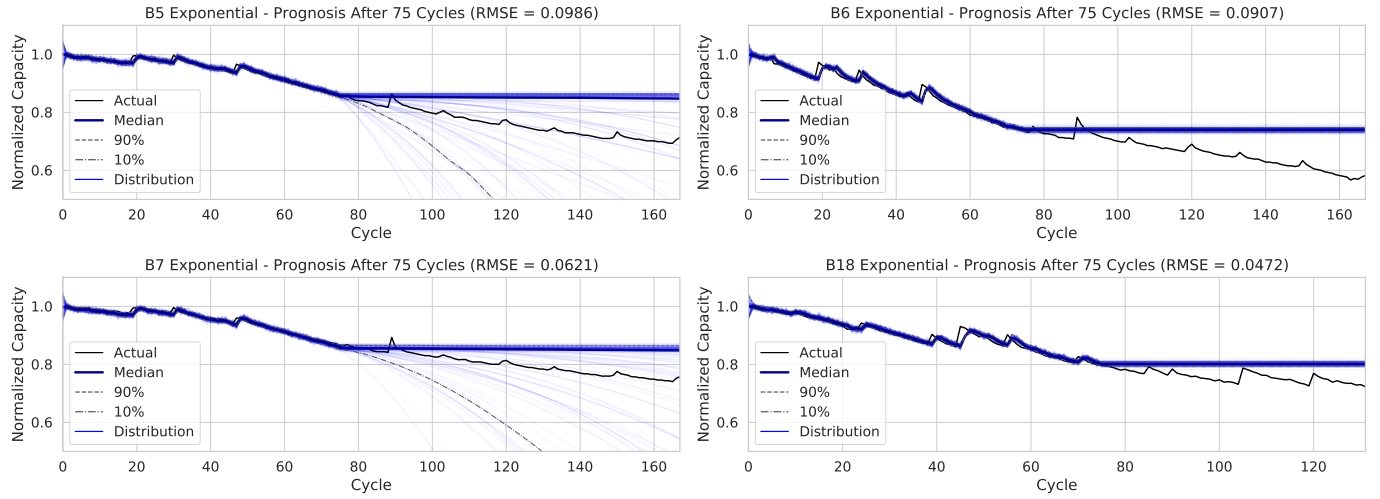


Fig. 4: Median PF RMSE examples for prognosis after 75 cycles using the gradual exponential model used in previous studies.

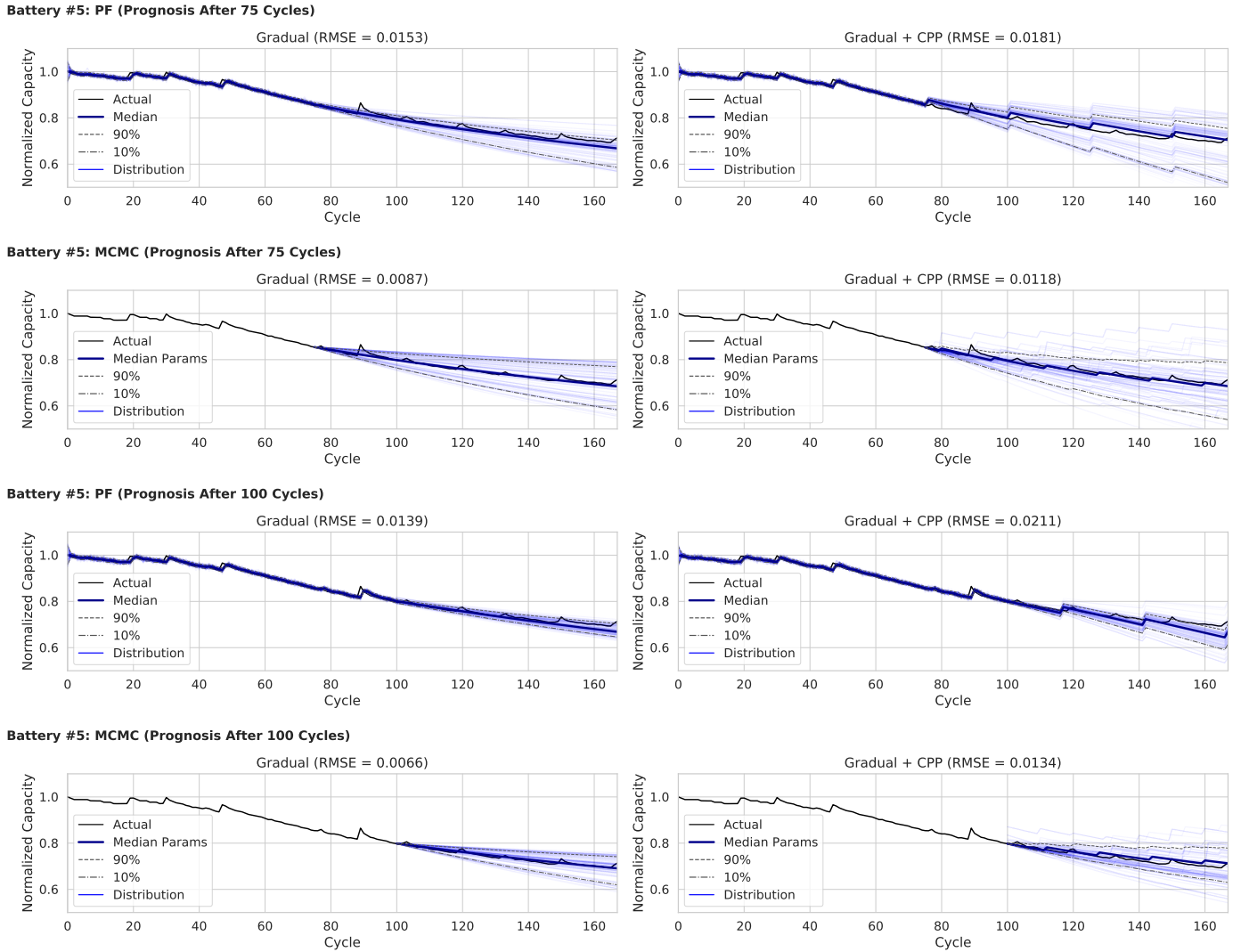


Fig. 5: Median RMSE examples of PF and MCMC for prognosis after 75 and 100 cycles with and without CPP for Battery #5

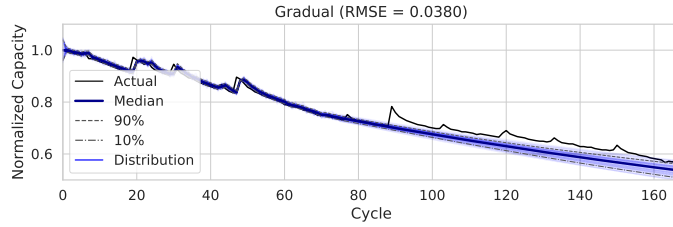
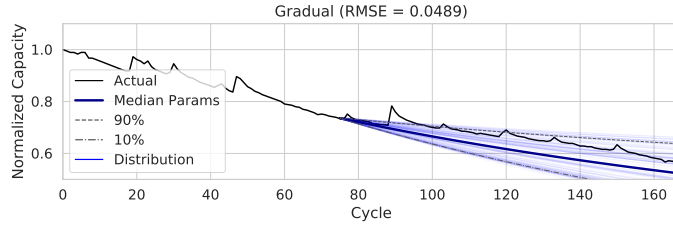
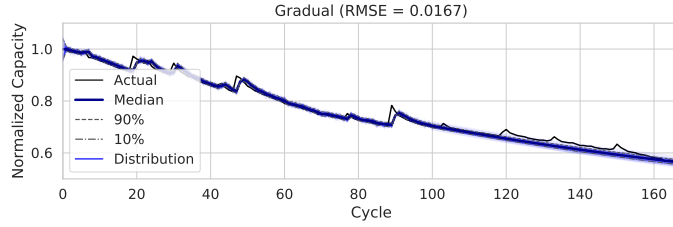
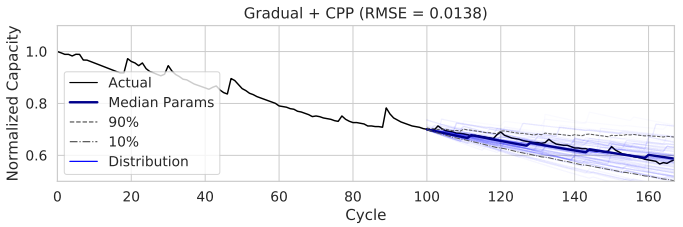
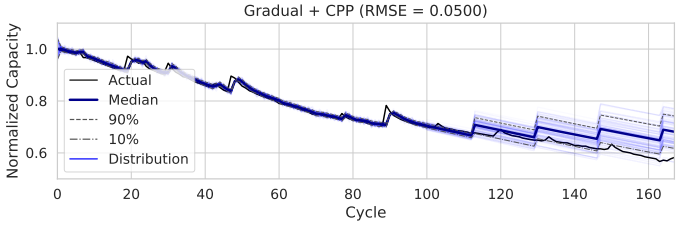
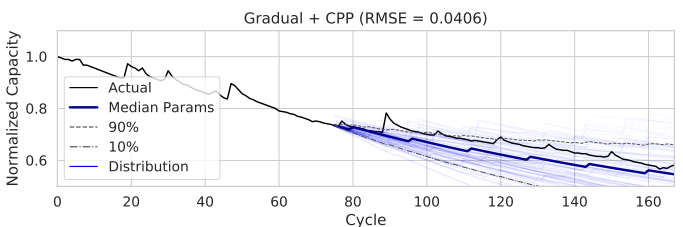
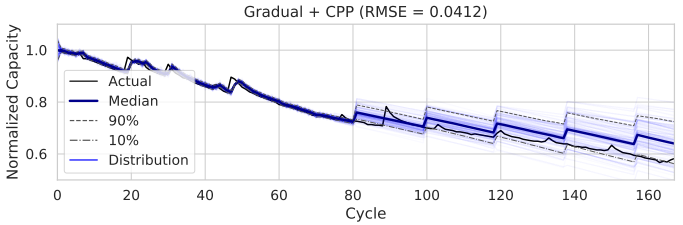
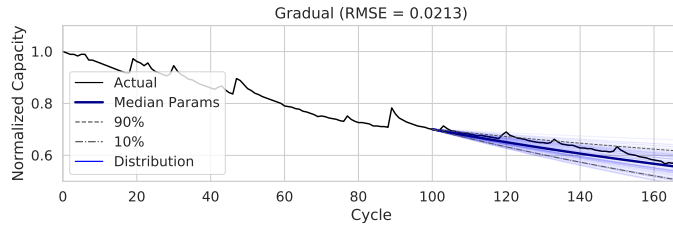
Battery #6: PF (Prognosis After 75 Cycles)**Battery #6: MCMC (Prognosis After 75 Cycles)****Battery #6: PF (Prognosis After 100 Cycles)****Battery #6: MCMC (Prognosis After 100 Cycles)**

Fig. 6: Median RMSE examples of PF and MCMC for prognosis after 75 and 100 cycles with and without CPP for Battery #6

is equivalently essential as the former evaluation metric. Along this line, future research will explore advanced statistical metrics that can better evaluate the prognosis results rather than just an average prediction error.

5.2. PF vs. MCMC

In most batteries and configurations, the MCMC prognosis outperforms PF prognosis according to the RMSE values in Figs. 5–8. The reasons are twofold. First, PF is a step-by-step estimation technique, while MCMC is a batch estimation technique. Compared to MCMC, PF projects the latest degradation trend instead of an overall degradation trend into prognosis. This would jeopardize the prognosis and result in worse performance, if the actual degradation trend varies largely before and after the time when the prognosis is made. Second, MCMC is demonstrated to be able to evaluate a multitude of CPP frequencies and magnitudes for a single battery rather than relying on point maximum likelihood estimates of these quantities. Thus,

the regeneration events would be generated adaptively for individual batteries by MCMC, better than using a fixed pattern to generate events in the prognosis by PF.

These results should be considered in light of the computational efficiency of MCMC and PF. Fig. 11 illustrates the dramatic difference in the time required to perform a single run of tracking and parameter estimation via MCMC as compared to the time needed for an equivalent level of data processing via PF. Tests were performed on an 2.1 GHz, 16-core Intel Xeon Gold 6130 CPU with 192 GB of RAM, and the PyTorch-based MCMC library Pyro [28] also leveraged an available NVIDIA Tesla V100 GPU with 24 GB of RAM. Averaged over 30 trials, PF estimated parameters from 75 cycles of data in 11 s, while MCMC required 520 s. With 100 cycles of input, PF averaged a completion time of 15 s, while MCMC finished processing in 690 s. It should be noted that the elapsed times compare the time required to process the same amount of data, not the time necessary to generate the same performance outcome (i.e., level of RMSE), which might require using multiple runs. Analyzing

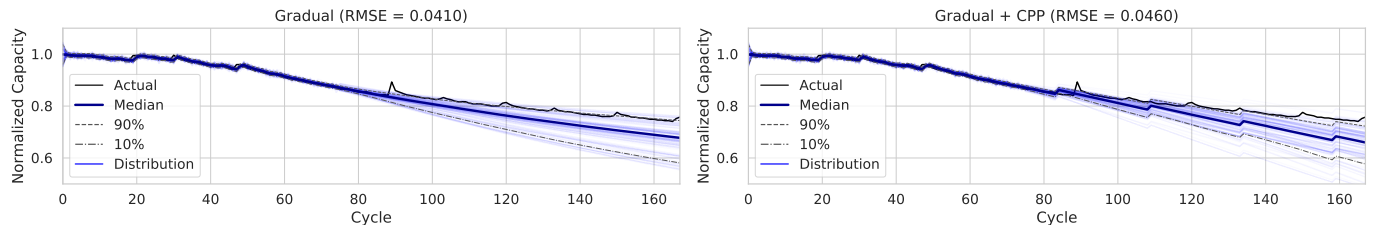
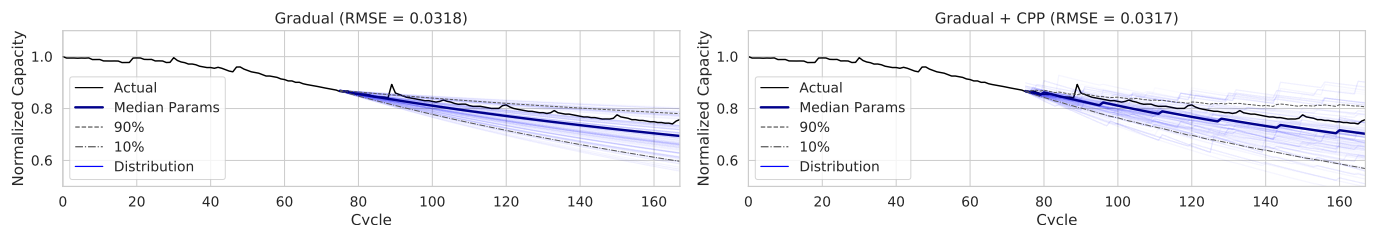
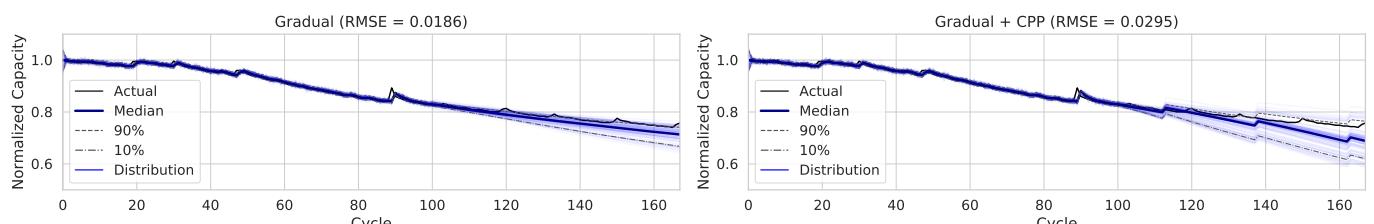
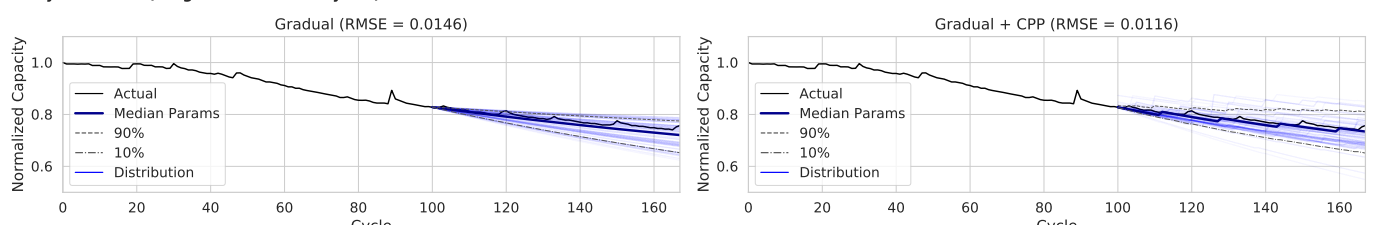
Battery #7: PF (Prognosis After 75 Cycles)**Battery #7: MCMC (Prognosis After 75 Cycles)****Battery #7: PF (Prognosis After 100 Cycles)****Battery #7: MCMC (Prognosis After 100 Cycles)**

Fig. 7: Median RMSE examples of PF and MCMC for prognosis after 75 and 100 cycles with and without CPP for Battery #7

the time needed to produce equivalent RMSE performance is left to a subsequent study.

In future research, the combination of PF and MCMC will be investigated. The hybrid estimation will leverage the step-by-step effectiveness of PF to track and estimate parameters of the gradual model, and retain MCMC for estimating CPP parameters. This approach can bring together the advantage of PF in capturing global and local fluctuations and the capability of MCMC in adaptively generating regeneration events. It will also allow for reducing the dimensionality of parameters estimated by MCMC, improving computational efficiency.

6. Summary

Motivated by the importance of lithium-ion battery degradation prognosis and RUL estimation, this paper presented a novel stochastic degradation model incorporating a rational polynomial approximation of gradual degradation and a CPP for characterizing the frequency and magnitude of transient regenera-

tion events. Incorporating regeneration event simulation critically ensures that future prognosis curves mirror the true behavior of the actual capacity evolution. Model parameters were estimated via two Bayesian methods, PF and MCMC, with and without the CPP for transient event simulation. Initial results indicate that MCMC-based estimation of the model with CPP generates realistic future prognosis curves with sufficient variation to capture the uncertainty in battery usage patterns. Future work combining PF and MCMC approaches can balance the tradeoff between MCMC-based performance and PF efficiency and tracking capability.

Acknowledgments

This study is supported by the seed grant funded by the University of Kentucky Energy Research Prioritization Partnership. We would thank the University of Kentucky Center for Computational Sciences and Information Technology Services Re-

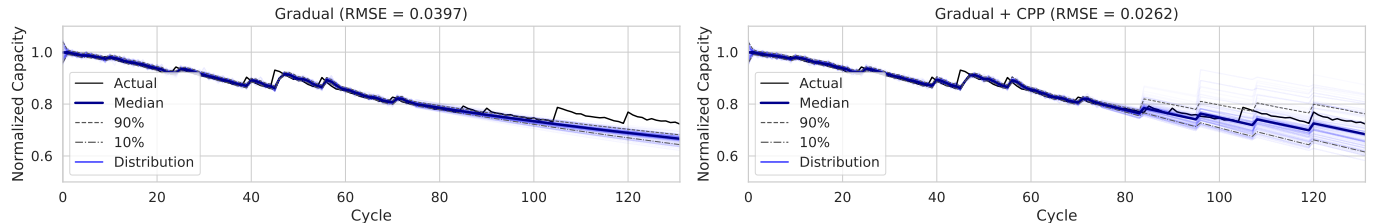
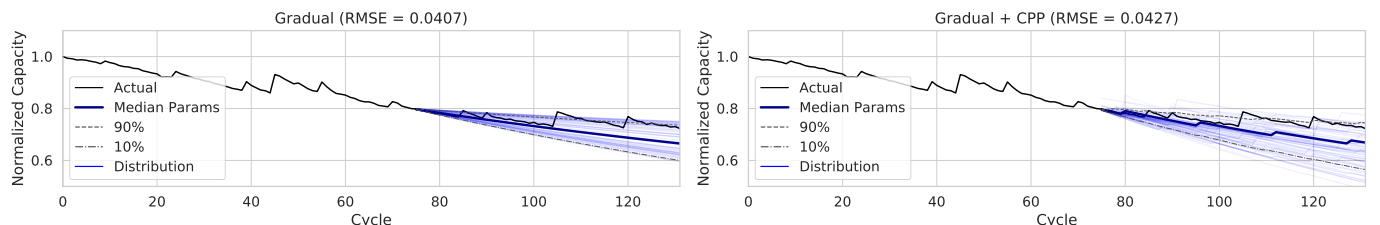
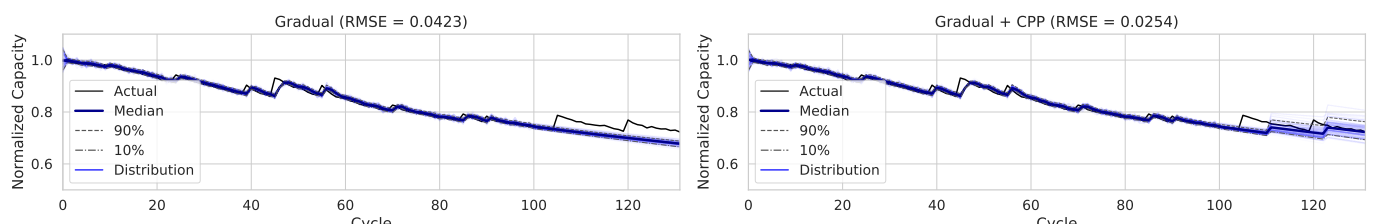
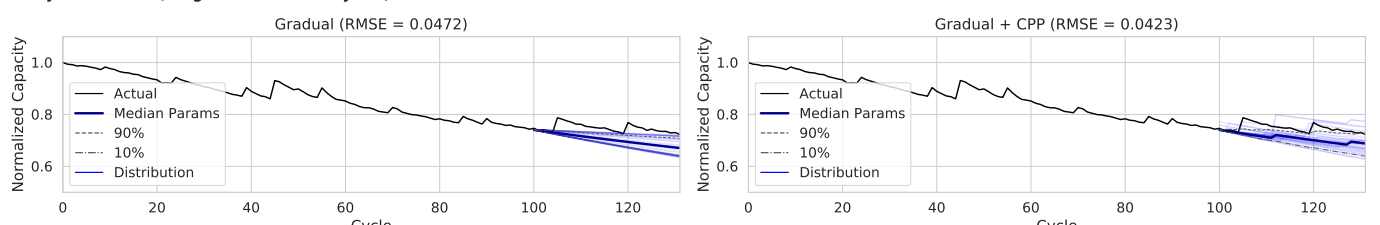
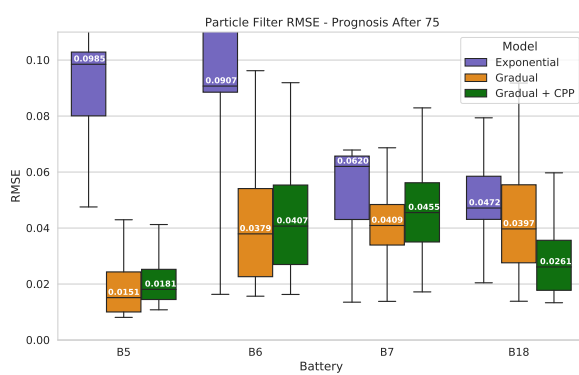
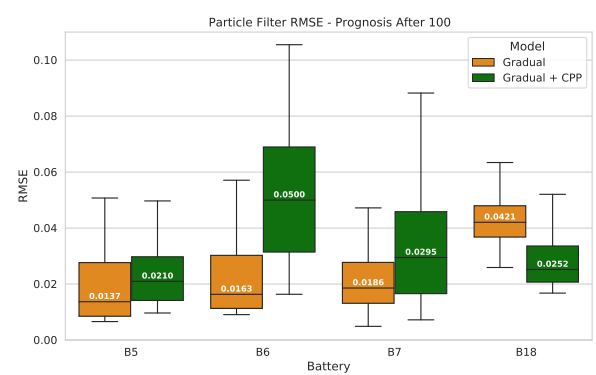
Battery #18: PF (Prognosis After 75 Cycles)**Battery #18: MCMC (Prognosis After 75 Cycles)****Battery #18: PF (Prognosis After 100 Cycles)****Battery #18: MCMC (Prognosis After 100 Cycles)**

Fig. 8: Median RMSE examples of PF and MCMC for prognosis after 75 and 100 cycles with and without CPP for Battery #18



(a)



(b)

Fig. 9: Prognosis RMSE using parameters estimated via particle filter over (a) 75 cycles and (b) 100 cycles.

search Computing for their support and use of the Lipscomb Compute Cluster and associated research computing resources.

References

- [1] Zhang, C., Li, K., Mcloone, S., Yang, Z., 2014. Battery modelling methods for electric vehicles - a review, pp. 2673–2678.

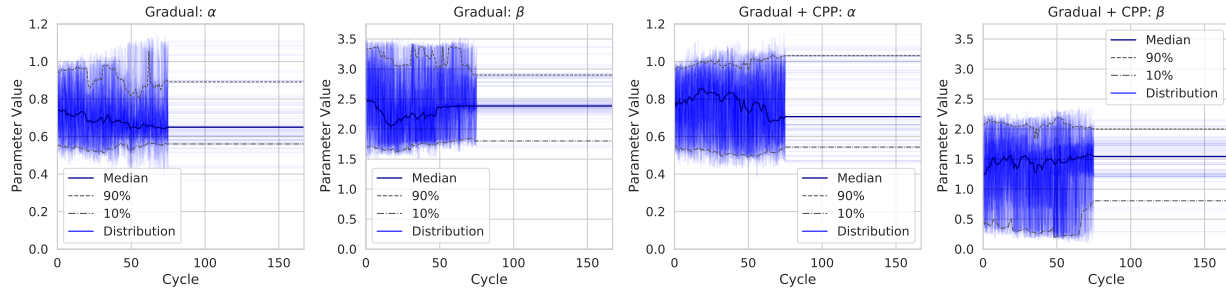


Fig. 10: Example of particle filter estimation of model parameters α and β for prognosis after 75 cycles on Battery 5.

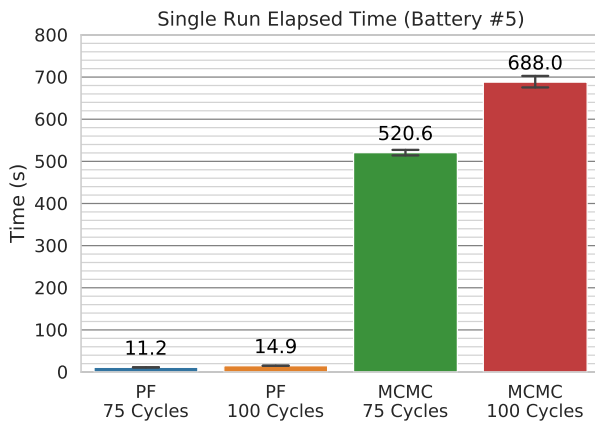


Fig. 11: Time required for a single run of MCMC or PF tracking for 75 and 100 cycles on Battery #5 (mean of 30 trials)

- [2] Gao, R., Wang, L., Teti, R., Dornfield, D., Kumara, S., Mori, M., Helu, M., 2015. Cloud-enabled prognosis for manufacturing. *CIRP Annals* 64, 749–772.
- [3] Downey, A., Lui, Y.H., Hu, C., Laflamme, S., Hu, S., 2019. Physics-based prognostics of lithium-ion battery using non-linear least squares with dynamic bounds. *Reliability Engineering and System Safety* 182, 1–12.
- [4] Zhao, G., Zhang, G., Liu, Y., Zhang, B., Hu, C., 2017. Lithium-ion battery remaining useful life prediction with deep belief network and relevance vector machine.
- [5] Qu, J., Liu, F., Ma, Y., Fan, J., 2019. A neural-network-based method for rul prediction and soh monitoring of lithium-ion battery. *IEEE Access* 7, 87178–87191.
- [6] Ren, L., Zhao, L., Hong, S., Zhao, S., Wang, H., Zhang, L., 2018. Remaining useful life prediction for lithium-ion battery: A deep learning approach. *IEEE Access* 6, 50587–50598.
- [7] Hartman II, R.L., 2008. An Aging Model for Lithium-Ion Cells. Ph.D. thesis. University of Akron.
- [8] Saha, B., Goebel, K., Christoffersen, J., 2009a. Comparison of prognostic algorithms for estimating remaining useful life of batteries. *Transactions of the Institute of Measurement and Control* 1, 293–308.
- [9] Saha, B., Goebel, K., Poll, S., Christoffersen, J., 2009b. Prognostics methods for battery health monitoring using a bayesian framework. *IEEE Transactions on Instrumentation and Measurement* 58, 291–296.
- [10] Liu, D., Luo, Y., Peng, Y., Peng, X., Pecht, M., 2012. Lithium-ion battery remaining useful life estimation based on nonlinear ar model combined with degradation feature. *Proceedings of the Annual Conference of the Prognostics and Health Management Society*.
- [11] Zhang, H., Mo, Z., Wang, J., Miao, Q., 2020. Nonlinear-drifted fractional brownian motion with multiple hidden state variables for remaining useful life prediction of lithium-ion batteries. *IEEE Transactions on Reliability* 69, 768–780.

- [12] Wang, P., Gao, R.X., 2019. Prognostic modeling of performance degradation in energy storage by lithium-ion batteries. *Procedia Manufacturing* 34, 911–920.
- [13] Zhang, Z.X., Si, X.S., Hu, C.H., Pecht, M.G., 2017. A prognostic model for stochastic degrading systems with state recovery: Application to li-ion batteries. *IEEE Transactions on Reliability* 66, 1293–1308.
- [14] Pang, X., Huang, R., Wen, J., Shi, Y., Jia, J., Zeng, J., 2019. A lithium-ion battery rul prediction method considering the capacity regeneration phenomenon. *Energies* 12, 2247.
- [15] Saha, B., Goebel, K., 2009. Modeling li-ion battery capacity depletion in a particle filtering framework. *Proceedings of the Annual Conference of the Prognostics and Health Management Society*.
- [16] He, W., Williard, N., Osterman, M., Pecht, M., 2011. Prognostics of lithium-ion batteries based on dempster-shafer theory and the bayesian monte carlo method. *Journal of Power Sources* 196, 10314–10321.
- [17] Li, L., Saldivar, A.A.F., Bai, Y., Li, Y., 2019. Battery remaining useful life prediction with inheritance particle filtering. *Energies* 12, 2784.
- [18] Chen, Y., He, Y., Li, Z., Chen, L., Zhang, C., 2020. Remaining useful life prediction and state of health diagnosis of lithium-ion battery based on second-order central difference particle filter. *IEEE Access* 8, 37305–37513.
- [19] Ross, S.M., 2019. The exponential distribution and the poisson process, in: Ross, S.M. (Ed.), *Introduction to Probability Models* (Twelfth Edition). twelfth edition ed.. Academic Press, pp. 293–374.
- [20] Wang, Z.Q., Hu, C.H., Si, X.S., Zio, E., 2018. Remaining useful life prediction of degrading systems subjected to imperfect maintenance: Application to draught fans. *Mechanical Systems and Signal Processing* 100, 802–813.
- [21] Wang, P., Gao, R.X., Woyczyński, W.A., 2020. Lévy process-based stochastic modeling for machine performance degradation prognosis. *IEEE Transactions on Industrial Electronics* (Early Access), 1–10.
- [22] Candy, J.V., 2007. Bootstrap particle filtering. *IEEE Signal Processing Magazine* 24, 73–85.
- [23] Metropolis, N., Rosenbluth, A., Rosenbluth, M., Teller, A., Teller, E., 1953. Equation of state calculations by fast computing machines. *Journal of Chemical Physics* 21, 1087–1092.
- [24] Duane, S., Kennedy, A.D., Pendleton, B.J., Roweth, D., 1987. Hybrid monte carlo. *Physical Letters B* 195, 216–222.
- [25] Neal, R.M., 2010. Mcmc using hamiltonian dynamics, in: Brooks, S., Gelman, A., Jones, G.L., Meng, X.L. (Eds.), *Handbook of Markov Chain Monte Carlo*. Chapman & Hall/CRC, pp. 113–162.
- [26] Hoffman, M.D., Gelman, A., 2014. The no-u-turn sampler: Adaptively setting path lengths in hamiltonian monte carlo. *Journal of Machine Learning Research* 15, 1593–1623.
- [27] Saha, B., Goebel, K., 2007. Battery Data Set. NASA Ames Research Center.
- [28] Bingham, E., Chen, J.P., Jankowiak, M., Obermeyer, F., Pradhan, N., Karaletsos, T., Singh, R., Szerlip, P., Horsfall, P., Goodman, N.D., 2018. Pyro: Deep Universal Probabilistic Programming. *Journal of Machine Learning Research* 20, 1–6.